



Short-Term Variability of Biological Production and CO₂ System Around Dongsha Atoll of the Northern South China Sea: Impact of Topography-Flow Interaction

Jen-Hua Tai¹, Wen-Chen Chou^{2,3*}, Chin-Chang Hung⁴, Kuan-Chieh Wu², Ying-Hsuan Chen², Tzong-Yueh Chen², Gwo-Ching Gong^{2,3}, Fuh-Kwo Shiah^{1,2} and Chun Hoe Chow⁵

OPEN ACCESS

Edited by:

Christian Lønborg,
Aarhus University, Denmark

Reviewed by:

Wei-dong Zhai,
Shandong University, China
Liang Xue,
First Institute of Oceanography,
Ministry of Natural Resources, China

*Correspondence:

Wen-Chen Chou
wcchou@mail.ntou.edu.tw

Specialty section:

This article was submitted to
Marine Biogeochemistry,
a section of the journal
Frontiers in Marine Science

Received: 20 November 2019

Accepted: 04 June 2020

Published: 26 June 2020

Citation:

Tai J-H, Chou W-C, Hung C-C,
Wu K-C, Chen Y-H, Chen T-Y,
Gong G-C, Shiah F-K and Chow CH
(2020) Short-Term Variability
of Biological Production and CO₂
System Around Dongsha Atoll of the
Northern South China Sea: Impact
of Topography-Flow Interaction.
Front. Mar. Sci. 7:511.
doi: 10.3389/fmars.2020.00511

¹ Research Center for Environmental Changes, Academia Sinica, Taipei, Taiwan, ² Institute of Marine Environment and Ecology, National Taiwan Ocean University, Keelung, Taiwan, ³ Center of Excellence for the Oceans, National Taiwan Ocean University, Keelung, Taiwan, ⁴ Department of Oceanography, National Sun Yat-sen University, Kaohsiung, Taiwan, ⁵ Department of Marine Environmental Informatics, National Taiwan Ocean University, Keelung, Taiwan

The short-term variabilities in temperature, salinity, nitrate, chlorophyll *a* (Chl *a*), and carbonate chemistry data (i.e., pH, partial pressure of CO₂ (*p*CO₂), total alkalinity, and dissolved inorganic carbon) were concurrently investigated in the shallow (~50 m) and deep (~300 m) water areas around Dongsha Atoll of the northern South China Sea (NSCS). The results show that surface temperature and *p*CO₂ were lower but that upward nitrate flux and Chl *a* were higher in the upper euphotic zone at the shallow-water area than those at the deep-water area. We suggest that the observed contrasting biogeochemical properties between the two areas could be attributed to the impact of topography-flow interaction. As tidal currents (or any other horizontal currents) interacted with the shallow topography, they may induce vertical isotherm displacements (e.g., internal tides/internal waves) that may enhance turbulent mixing, and thus can transport more nutrient-replete subsurface water into the euphotic zone and stimulate phytoplankton production. The stimulated biological production and the cooling effect induced by topography-flow interaction may collectively drive surface *p*CO₂ down in the shallow water area. Though the present short-term hydrological and CO₂ data, which to our knowledge were concurrently investigated for the first time in the NSCS, reveal that the topography-flow interaction could be a favorable mechanism for atmospheric CO₂ uptake around Dongsha Atoll, more long-term observations are still needed to confirm that the similar processes can repetitively take place in topography-flow interaction prevalent areas.

Keywords: topography-flow interaction, internal tides, internal waves, carbon dioxide, chlorophyll-a, nutrients, Dongsha Atoll, South China Sea

INTRODUCTION

It has been suggested that interaction between submarine relief (e.g., seamounts and islands) and local currents may induce localized uplifting of isotherms and possibly stronger mixing, which would favor the transfer of nutrients from deeper to shallower waters, and thus support higher phytoplankton production when compared to the surrounding ocean, especially in the oligotrophic waters of the subtropics (Rowden et al., 2010; Read and Pollard, 2017). For example, de Souza et al. (2013) reported that topography-flow interaction has created a patchy pattern of Chlorophyll *a* (Chl *a*) and nutrient distribution around the islands and seamounts of the tropical south-western Atlantic.

Dongsha Atoll is a remote coral reef, located at the edge of the continental shelf in the oligotrophic northern South China Sea (NSCS; Liu et al., 2007). Previous studies have revealed that the Chl *a* concentration in the shallow-water area around Dongsha Atoll was higher than that in the surrounding ocean (Wang et al., 2007; Pan et al., 2012) suggesting the enhancement of biological production through the interaction between topography and local currents (such as tidal currents), which can produce intensive internal tides/waves (ITs/IWs) in the NSCS (Liu et al., 1998; Zhao et al., 2004; Alford et al., 2015). Chen et al. (2016) further indicated that the nutrient pulses driven by the uplifting of isotherms induced by topography-flow interaction may not only stimulate phytoplankton primary production but also enhance heterotrophic bacterial growth. These studies have shown robust correlations between the increase in primary production and the topography-flow interaction, and as a result, one may speculate that oceanic CO₂ uptake may be enhanced as well. However, to our knowledge, the potential impacts of topography-flow interaction on the biological production and surface CO₂ system have never been concurrently investigated in the NSCS.

In this study, we concurrently investigated the short-term variabilities in hydrological factors (i.e., temperature, salinity, nitrate, and Chl *a*) and carbonate chemistry data [i.e., pH, partial pressure of CO₂ (*p*CO₂), total alkalinity (TA), and dissolved inorganic carbon (DIC)] at two distinct anchored stations around Dongsha Atoll of the NSCS. One station is located in the shallow-water area with a bottom depth of ~50 m on the east coast off Dongsha Atoll; the other is situated in the deep-water area with a bottom depth of ~300 m in the northeast ~30 km off Dongsha Atoll (Figure 1). Since the water mixing between the subsurface and the surface mixed-layer induced by the topography-flow interaction is more prominent in the shallow-water area than in the deep-water area (Jan and Chen, 2009; Read and Pollard, 2017), we hypothesized that the upward nitrate flux and Chl *a* concentrations would be elevated, while the *p*CO₂ would be depressed at the shallow-water station compared with those at the deep-water station. More importantly, while the effect of topography-flow interaction on biological production has been extensively studied (Sandstrom and Elliott, 1984; Sharples et al., 2009; de Souza et al., 2013; Villamaña et al., 2017), the concomitantly measured CO₂ data are still unavailable. Therefore, the present study provides us a rare opportunity to simultaneously examine the potential impact

of the topography-flow interaction on the biological production and subsequent CO₂ dynamics.

MATERIALS AND METHODS

High Frequency Measurements of Temperature, pH and *p*CO₂, and Vertical Profiles of Temperature, Salinity, and Chl *a*

At each station, a moored buoy was deployed to record high-frequency variations in temperature, pH and *p*CO₂ for a period of 28 h (from 07:00 September 4 to 11:00 September 5, 2018) at the shallow-water station (~50 m; DS) and for a period of 26 h (from 17:00 September 5 to 19:00 September 6, 2018) at the deep-water station (~300 m; K2). The configurations of the moored buoys deployed at the two stations are shown and described in **Supplementary Figure 1**. The interval of the measurements for temperature, pH and *p*CO₂ was 1, 10, and 15 min, respectively. The vertical distributions of temperature and salinity were recorded by CTD (SeaBird 9/11-plus) every two hours. In order to avoid the risk of coiling between the mooring and the CTD cables, the hydrological station has been kept a safe distance away from the mooring station. The distance between the mooring and hydrological stations is less than 500 m. Concentrations of Chl *a* were measured by a fluorometer (Cleave Aua tracka III) attached to the CTD to monitor vertical profiles of fluorescence, which was calibrated by in situ Chl *a* measurements by a Turner Designs fluorometer (10-AU-005) after extraction with 90% acetone using a nonacidification method (Gong et al., 1996).

DIC, TA, pH, and Nitrate Measurements of Discrete Water Samples

Discrete water samples for the determinations of DIC, TA, pH, and nitrate were collected by Go-Flo bottles mounted onto a rosette sampling assembly every 4 h at six depths of 2, 10, 25, 50, and 75 and ~5 m above the bottom at the DS station and 150 m at the K2 station. The methods for the DIC, TA and pH analyses were described by Chou et al. (2016) and references therein. Briefly, the DIC and TA were determined using the nondispersive infrared method on a DIC analyzer (AS-C3, Apollo SciTech) and Gran titration on an automatic TA titrator (AS-ALK2, Apollo SciTech), respectively, and both measurements had accuracies and precisions of 0.15% ($\pm 3 \mu\text{mol kg}^{-1}$) or better. The pH was spectrophotometrically measured with a precision of 0.001. The concentration of nitrate was analyzed by the pink azo dye method based on Gong et al. (1996) with a precision of $\pm 0.3 \mu\text{M}$.

RESULTS

Short-Term Variabilities of Temperature, *p*CO₂ and pH

The high frequency variations of temperature (1 min) at various depths and *p*CO₂ (15 min) and pH (10 min) at the surface (2 m) recorded by the mooring sensors are shown in

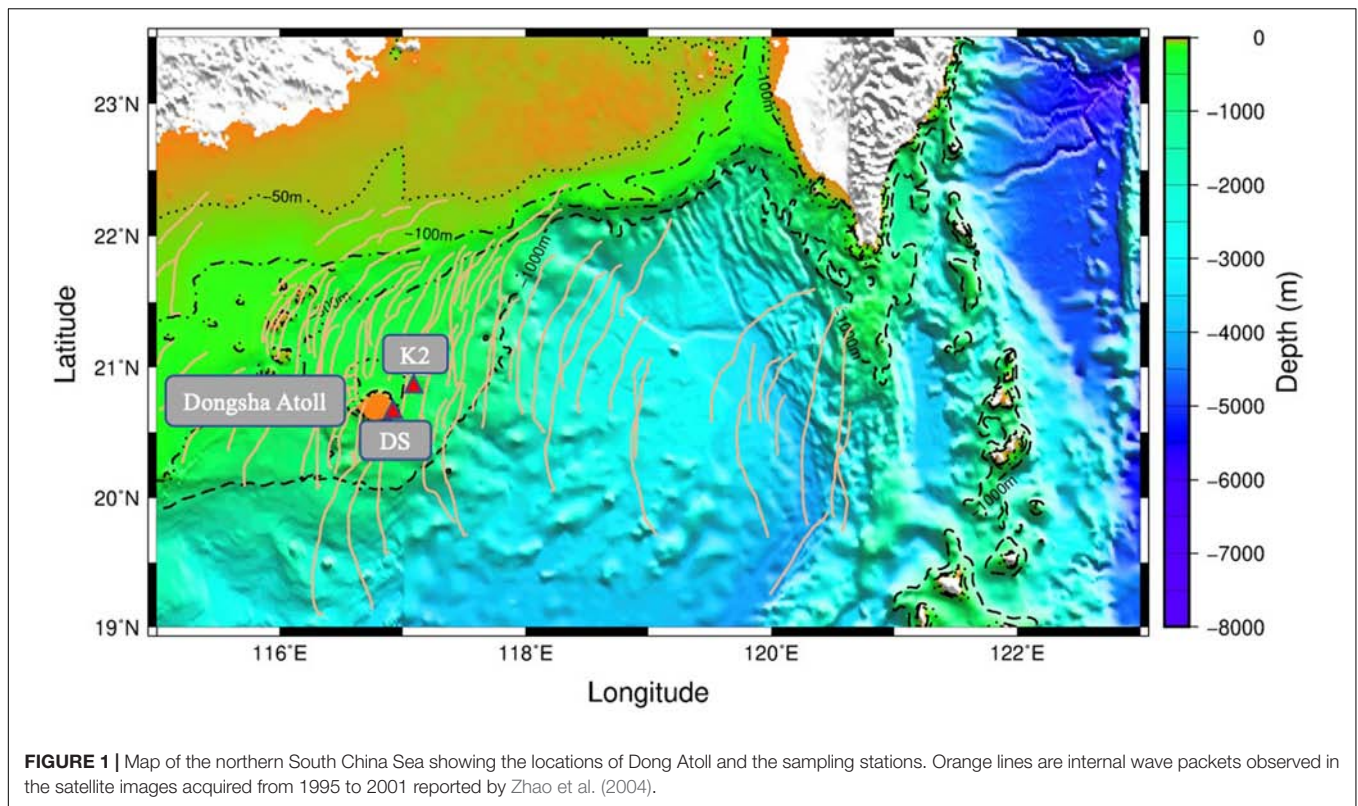


Figure 2. Large variations in temperature were observed in the subsurface layer (~20–120 m) at both stations, signifying the vertical isotherm displacements (also suggesting the possible occurrence of ITs/IWs), which could be induced by the topography-flow interaction (such as tidal currents or any other horizontal currents). For example, a sudden undulation of water temperature up to $\sim 5.7^{\circ}\text{C}$ was found at 45 m at the DS station (pink line in **Figure 2A**), in which water temperature increased from ~ 22.1 to $\sim 27.8^{\circ}\text{C}$ at 9 pm on 4th September to 1 am on 5th September. In addition to this major event, there were 6–7 minor temperature oscillation events with smaller amplitudes between 2.0 and 4.0°C during the mooring period at the DS station. At the K2 station, a sharp temperature oscillation up to $\sim 8.0^{\circ}\text{C}$ was observed at 60 m (pink line in **Figure 2B**), in which the water temperature increased from ~ 20.3 to $\sim 28.3^{\circ}\text{C}$ from 7 to 10 am on 6th September (**Figure 2B**). However, in comparison to the DS station, a smaller number of temperature undulation events were observed at the K2 station. Overall, the observed elongated and more temperature oscillation events at the DS station are consistent with the extensive occurrence of vertical isotherm displacements in shallow-water areas induced by the topography-flow interaction (Fu et al., 2012). Therefore, in comparison to the deep-water K2 station, the turbulent processes at the shallow-water DS station should be enhanced.

Unlike the large temperature variations observed in the subsurface layer, sea surface temperature (SST) varied within a relatively narrow range from 27.9 to 28.9°C at the DS station and from 28.4 to 29.9°C at the K2 station (**Figures 2C,D**). The average SST was significantly lower at the DS station than

at the K2 station by $\sim 0.7^{\circ}\text{C}$ ($28.7 \pm 0.2^{\circ}\text{C}$ vs. $29.4 \pm 0.3^{\circ}\text{C}$; $p < 0.001$, **Supplementary Table 1**), suggesting a stronger cooling effect in the shallow-water area induced by the enhancement of vertical mixing between the subsurface and the surface mixed-layer. Surface $p\text{CO}_2$ and pH ranged from 348 to 381 μatm and 8.01 to 8.05 at the DS station, and from 368 to 395 μatm and 8.00 to 8.03 at the K2 station, respectively (**Figures 2E–H**). In terms of average values, $p\text{CO}_2$ was lower, and the pH was higher at the DS station than those at the K2 station (362 ± 7 vs. 383 ± 6 μatm and 8.03 ± 0.01 vs. 8.01 ± 0.00 , respectively; $p < 0.001$, **Supplementary Table 1**). The lower average $p\text{CO}_2$ and higher average pH at the DS station may reflect the fact that increased photosynthetic CO₂ consumption was fueled by the nutrient supply through the stronger vertical mixing, which will be further examined in section “Discussion”.

Depth Distributions of Temperature, Salinity, DIC, TA, pH, Nitrate, and Chl *a* During the Upward and Downward Phases of Isotherm Displacements

The temporal variations in the depth distributions of temperature, salinity, Chl *a*, nitrate, DIC, TA, pH at the DS and K2 stations are shown in **Supplementary Figure 2**. Based on the undulations of isotherms of 25°C shown in **Supplementary Figures 2a,b**, the water column properties measured at 11 am on 4th September and 3 am on 5th September were chosen to represent the typical vertical hydrographic settings during the downward phases of isotherm displacements, and those at 3 pm

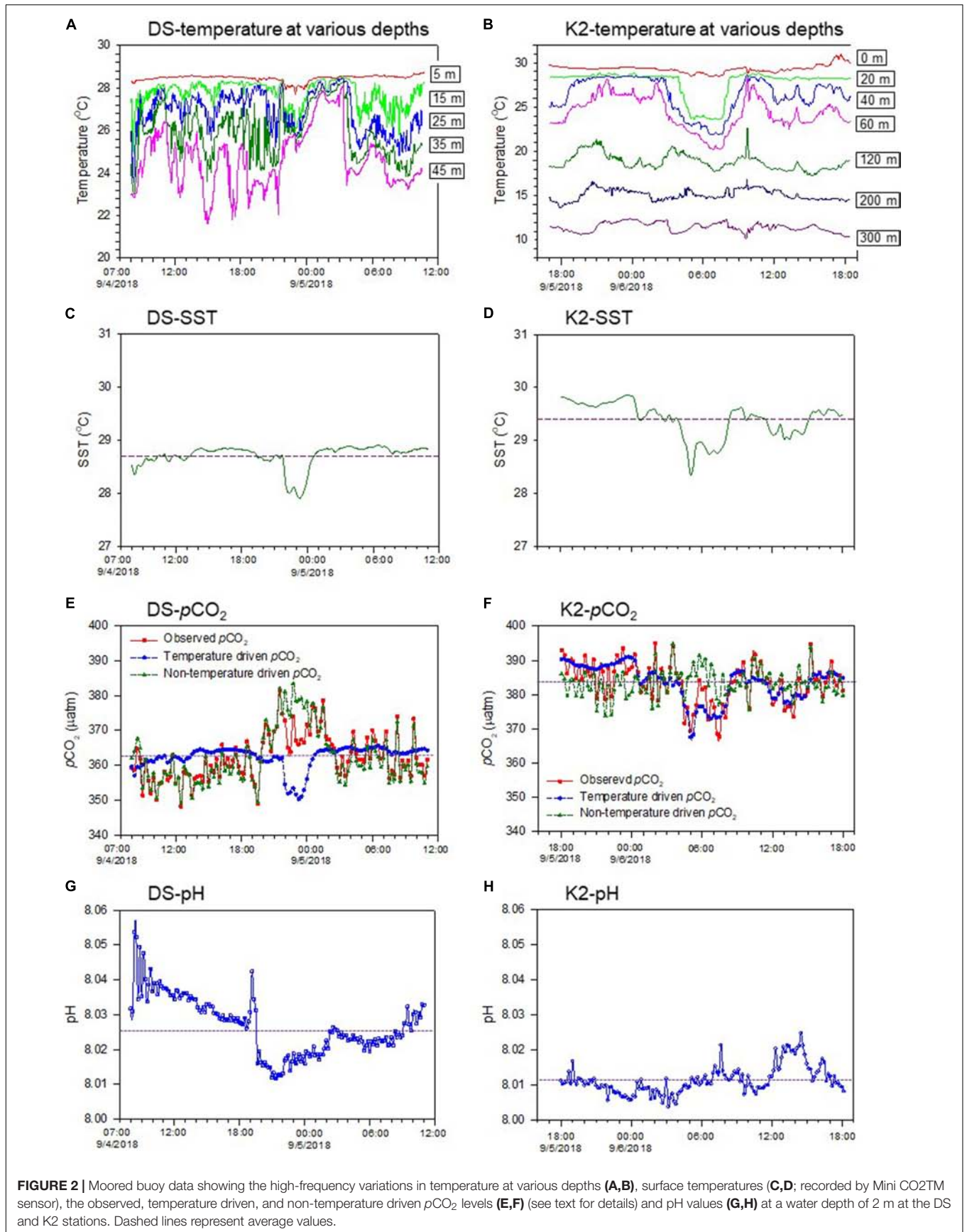


FIGURE 2 | Moored buoy data showing the high-frequency variations in temperature at various depths (A,B), surface temperatures (C,D; recorded by Mini CO2TM sensor), the observed, temperature driven, and non-temperature driven pCO₂ levels (E,F) (see text for details) and pH values (G,H) at a water depth of 2 m at the DS and K2 stations. Dashed lines represent average values.

on 4th September and 7 am on 5th September were used to stand for the typical setting during the upward phases of isotherm displacements at the DS station. For the K2 station, the typical vertical hydrographic settings during the downward and upward phases were denoted by the measurements conducted at 10 pm on 5th September and 6 am on 6th September, respectively.

The comparison of the vertical distributions in temperature, salinity, Chl *a*, nitrate, DIC, TA and pH between the upward and downward phases at the DS and K2 stations are shown in **Figure 3**. The hydrological factors and carbonate chemistry parameters generally showed relatively minor variations in the surface mixed-layer (defined as the surface layer with a potential density variation less than 0.1 kg m^{-3} ; the average depth was indicated by green dashed-line in **Figure 3**), while large variations were found in the lower euphotic zone (the depth interval between the bottoms of the mixed-layer and euphotic zones, defined as the depth of 0.1% surface light penetration; the average depth was indicated by gray solid-line in **Figure 3**) between the upward and downward phases of isotherm displacements. As shown in **Figures 3G,H**, nitrate generally remained under the detection limit ($<0.1 \mu\text{M}$) in the mixed layer, while it noticeably increased in the lower euphotic zone between the downward and upward phases at the both stations. The subsurface Chl *a* maximum depth (SCMD) revealed a distinct vertical movement between the downward and upward phases, moving from ~ 60 to ~ 40 m and from ~ 105 to ~ 60 m at the DS and K2 stations (**Figures 3E,F**), respectively. The other hydrological and carbonate parameters also revealed substantial variations in the lower euphotic zone, in which salinity, DIC and TA were higher, but temperature and pH were lower during the upward phase than those during the downward phase. The observed large variations clearly demonstrate that vertical isotherm displacements may largely influence the biogeochemical setting of the lower euphotic zone.

DISCUSSION

Comparison of Integrated Nitrate and Chl *a* Inventories Between the Upward and Downward Phases of Isotherm Displacements

In order to examine if phytoplankton can immediately respond to the newly upwelled nutrients during the upward phases of isotherm displacements induced by the topography-flow interaction, we have integrated the nitrate and Chl *a* inventories throughout the water column for the DS station (0–80 m) and from surface to 150 m for the K2 station (noting that there is virtually no Chl *a* below 150 m), during the upward and downward phases (**Figures 4A–D**). The calculated results show that the integrated nitrate inventory was elevated during the upward phases compared with that during the downward phase at the DS station (232.0 ± 80.1 vs. $118.9 \pm 35.3 \text{ mmol m}^{-2}$; **Figure 4A**), while the integrated Chl *a* inventory did not reveal a corresponding increase (20.6 ± 1.2 vs. $20.6 \pm 2.6 \text{ mg m}^{-2}$; **Figure 4B**). A similar case was observed at the K2 station

with a higher nitrate inventory of $667.8 \text{ mmol m}^{-2}$ during the upward phase and a lower inventory of $328.5 \text{ mmol m}^{-2}$ during the downward phase (**Figure 4C**), whereas the integrated Chl *a* inventory did not show a significant difference between the two phases (23.0 vs. 25.6 mg m^{-2} ; **Figure 4D**). The observed divergent responses of the integrated nitrate and Chl *a* inventories between the upward and downward phases suggest that biological production may need longer time to response the newly nutrient supply induced by the vertical isotherm displacements.

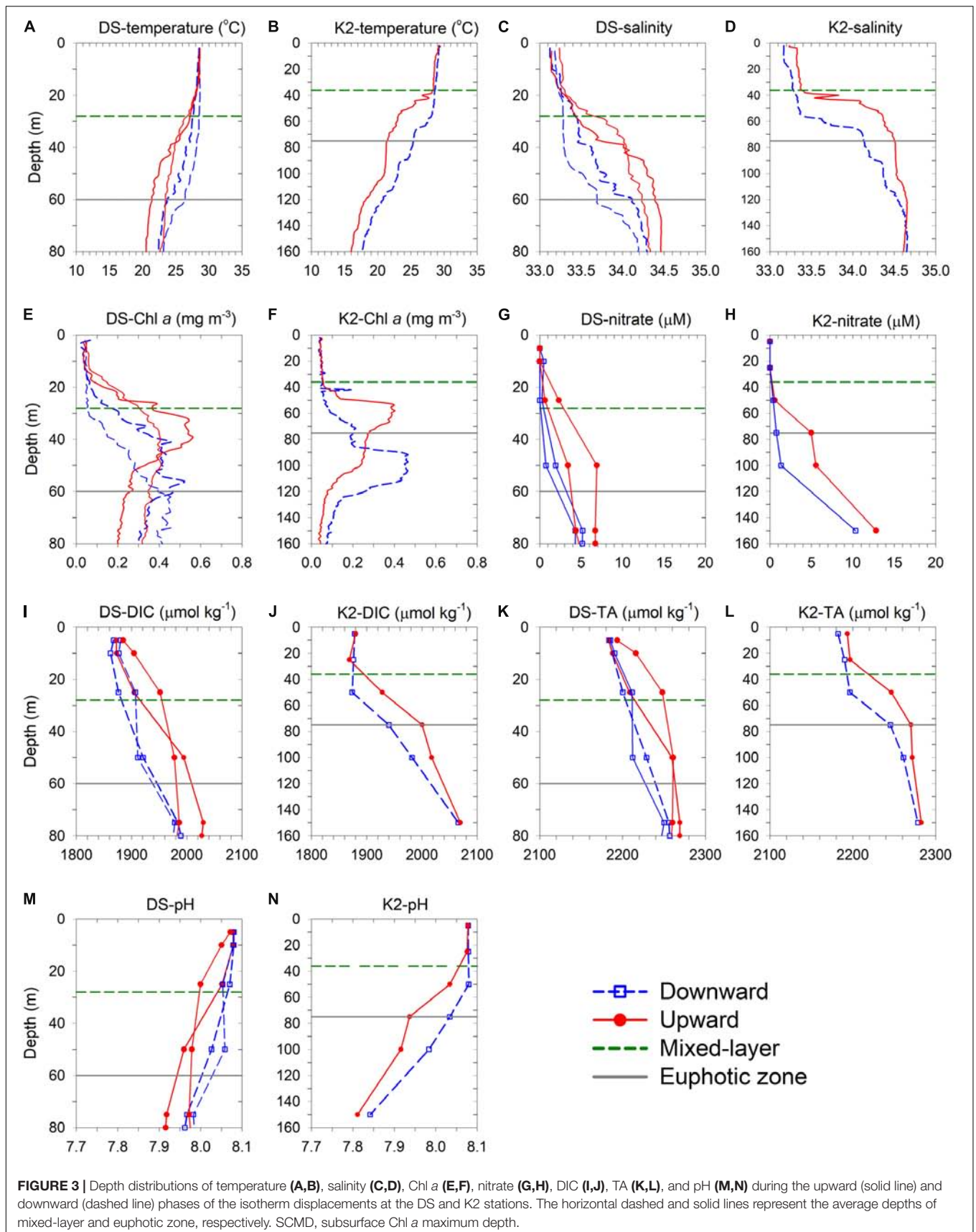
Comparison of Upward Nutrient Flux and Chl *a* Concentration Between the Shallow-Water (DS) and Deep-Water (K2) Stations

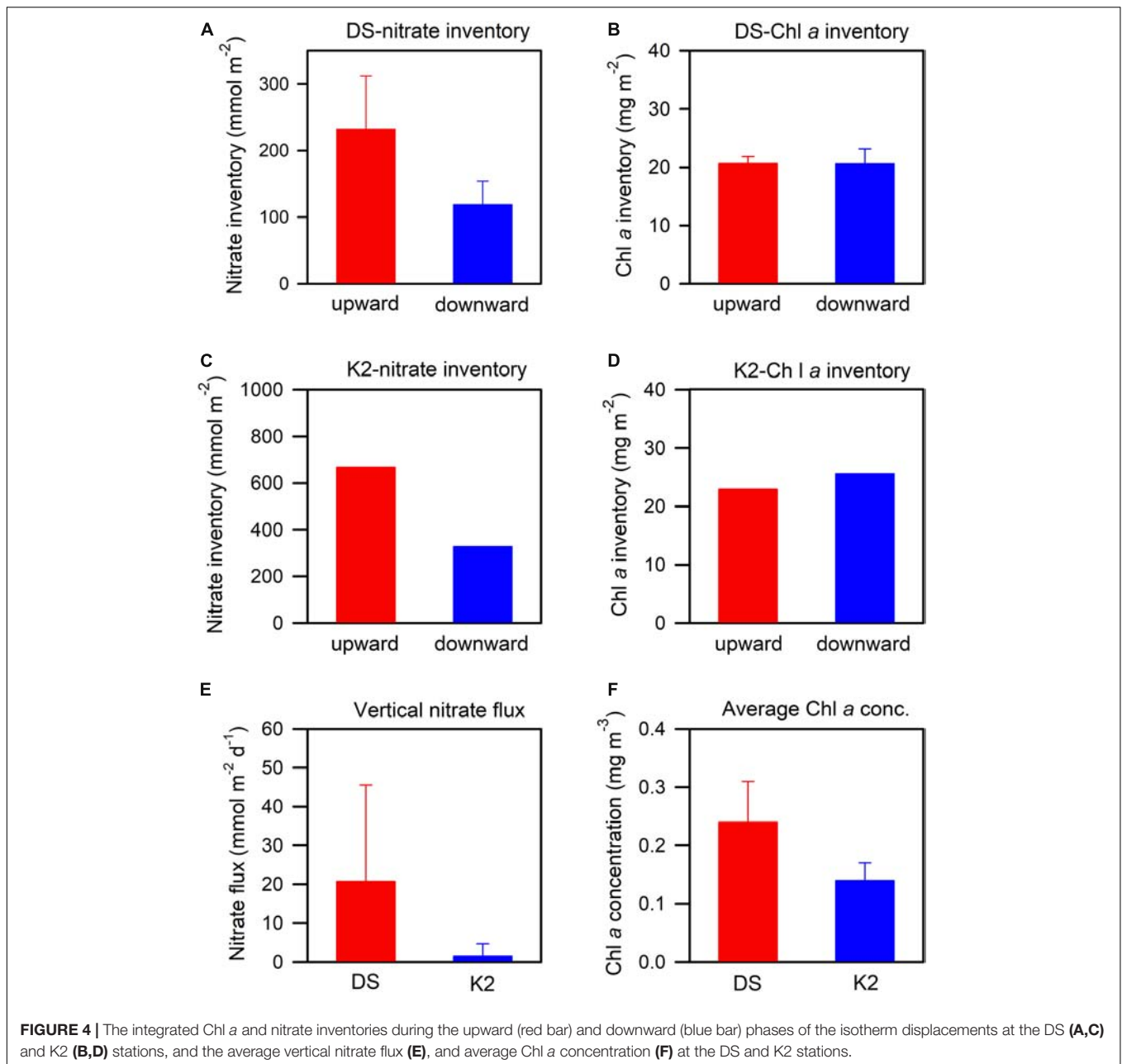
Although the comparison of the integrated nitrate and Chl *a* inventories between the upward and downward phases of isotherm displacements suggest that phytoplankton could not immediately respond to the newly upwelled nutrients, it does not necessarily mean that vertical isotherm displacements induced by the topography-flow interaction did not exert a control on the biological production. To better understand how nutrient supply may affect Chl *a* concentration in the euphotic zone, we applied a simple diffusion model to calculate the average upward nutrient flux during the study period at the two stations (Li et al., 2018). The average nitrate gradient below the SCMD was estimated to be 0.097 ± 0.028 and $0.105 \pm 0.011 \text{ mmol m}^{-4}$ at the DS and K2 stations, respectively. The average diffusivity rate was $(3.2 \pm 4.5) \times 10^{-3}$, and $(1.9 \pm 3.8) \times 10^{-4} \text{ m}^2 \text{ s}^{-1}$, respectively, estimated from the potential density profiles following Frants et al. (2013). The resultant upward diffusion flux of nitrate was 20.74 ± 24.81 and $1.56 \pm 3.07 \text{ mmol m}^{-2} \text{ d}^{-1}$ at the DS and K2 stations, respectively (**Figure 4E**). This estimation clearly demonstrates that the nutrient supply at the shallow-water DS station could be one order of magnitude higher than the deep-water K2 station.

Corresponding to the higher upward flux of nitrate at the shallow water area, the average Chl *a* concentration above the SCMD was estimated to be $0.24 \pm 0.07 \text{ mg m}^{-3}$ at the DS station, which was approximately 2 times higher than that at the K2 station ($0.14 \pm 0.03 \text{ mg m}^{-3}$; **Figure 4F**). These results clearly reveal that the vertical isotherm displacement induced by topography-flow interaction may lead to stronger vertical mixing in the shallow-water area than in the deep-water area, which may result in more nutrient-replete subsurface water into the euphotic zone and thus stimulate phytoplankton production.

Lower Surface pCO₂ at the Shallow-Water DS Station and Potential Mechanisms

As evidenced by the comparison between the shallow and deep water stations, the recurring vertical isotherm displacements induced by topography-flow interaction in the shallow water area is a favorable mechanism to stimulate biological production. In the following, we will further examine if oceanic CO₂ uptake may





be also enhanced in response to the high biological production in the shallow water area. Since $p\text{CO}_2$ is temperature dependent with a rate of $\sim 4\% \text{ } ^\circ\text{C}^{-1}$ (Takahashi et al., 1993) the cooling effect associated with the recurring vertical isotherm displacements (i.e., the average SST was $\sim 0.7^\circ\text{C}$ lower at the DS station than at the K2 station) may have caused the decrease in $p\text{CO}_2$ of $\sim 10 \mu\text{atm}$, which could only account for $\sim 50\%$ of the observed $p\text{CO}_2$ reduction between K2 and DS stations, suggesting that the stimulated biological production may also partially contribute to the observed lower $p\text{CO}_2$ at the shallow water station.

To better understand the processes controlling the observed variation in surface $p\text{CO}_2$, we have calculated the temperature driven $p\text{CO}_2$ and non-temperature driven $p\text{CO}_2$ using the

method proposed by Takahashi et al. (2002) (see **Supplementary Method** for details). The calculated results show that the observed $p\text{CO}_2$ (red symbols) generally follows the non-temperature driven $p\text{CO}_2$ (green symbols) at the DS station (**Figure 2E**), while it tends to track the temperature driven $p\text{CO}_2$ (blue symbols) at the K2 station (**Figure 2F**). The relationships between $p\text{CO}_2$ and temperature at the DS and K2 stations are further examined in **Supplementary Figure 3**. As shown, a strong positive correlation was found for the K2 station ($r = 0.76$; red dashed line), which is consistent with the theoretically thermodynamic relationship between $p\text{CO}_2$ and temperature (green solid line). This agreement further supports that temperature could be the predominant factor controlling surface $p\text{CO}_2$ variation at the

K2 station. In fact, the dominance of temperature effect on surface $p\text{CO}_2$ variation is a ubiquitous phenomenon in global oligotrophic open oceans (Rogers, 1994; Bates et al., 1996; Winn et al., 1998; Takahashi et al., 2002). This commonality thus implies that the vertical isotherm displacement in the deep-water area may not exert a strong control on the variation in surface $p\text{CO}_2$. In contrast to the strong correlation at the K2 station, $p\text{CO}_2$ was poorly correlated with temperature at the DS station ($r = 0.10$). Moreover, most of the measured data fell below the thermodynamic relationship. The poor correlation and the deficiency in the measured $p\text{CO}_2$ relative to the theoretically temperature-dependent values imply that some factor(s) other than temperature play an important role in regulating $p\text{CO}_2$ variation at the DS station, and that the factor(s) should be able to simultaneously cause CO₂ removal from surface waters. The controlling factors other than temperature include biological processes, air-sea CO₂ exchange, and vertical mixing of subsurface water. Because both vertical mixing of subsurface water and air-sea CO₂ exchange would result in surface $p\text{CO}_2$ increase (noting that the observed $p\text{CO}_2$ was lower than atmospheric $p\text{CO}_2$ ($\sim 400 \mu\text{atm}$), hence CO₂ gas would penetrate into surface ocean from the atmosphere), the remaining observed lower surface $p\text{CO}_2$ at the DS station could be only attributed to the enhanced biological production fueled by the higher upward diffusion flux of nutrients at the shallow water area.

In summary, the present study concurrently investigated the short-term variability of hydrological factors and CO₂ system in the shallow and deep water areas in the NSCS for the first time. The results show that the vertical isotherm displacements induced by the topography-flow interaction in the shallow water area may stimulate biological production and decrease temperature, which may collectively drive surface $p\text{CO}_2$ down, and thus could be favorable for oceanic CO₂ uptake. Since this study only collected data during a diurnal cycle at each stations, more long-term observations (several months to 1 year) are still needed to confirm that the similar processes can repetitively take place in in topography-flow interaction prevalent areas.

REFERENCES

- Alford, M. H., Peacock, T., MacKinnon, J. A., Nash, J. D., and Buijsman, M. C. (2015). The formation and fate of internal waves in the South China Sea. *Nature* 521, 65–69.
- Bates, N. R., Michaels, A. F., and Knap, A. H. (1996). Seasonal and interannual variability of oceanic carbon dioxide species at the U.S. JGOFS Bermuda Atlantic-series Study (BATS) site. *Deep Sea Res. II* 43, 347–383. doi: 10.1016/0967-0645(95)00093-3
- Chen, T.-Y., Tai, J.-H., Ko, C.-Y., Hsieh, C.-H., and Chen, C.-C. (2016). Nutrient pulses driven by internal solitary waves enhance heterotrophic bacterial growth in the South China Sea. *Environ. Microbiol.* 18, 4312–4323. doi: 10.1111/1462-2920.13273
- Chou, W.-C., Gong, G.-C., Yang, C.-Y., and Chuang, K.-Y. (2016). A comparison between field and laboratory pH measurements for seawater on the East China Sea shelf. *Limnol. Oceanogr. Methods* 14, 315–322. doi: 10.1002/lom3.10091
- de Souza, C. S., da Luz, J. A. G., Macedo, S., Montes, M., and de, J. F. (2013). Chlorophyll a and nutrient distribution around seamounts and islands of the tropical south-western Atlantic. *Mar. Freshw. Res.* 64, 168–184.
- Frants, M., Damerell, G. M., Gille, S. T., Heywood, K. J., Mackinnon, J., and Sprintall, J. (2013). An assessment of density-based finescale methods for estimating diapycnal diffusivity in the Southern Ocean. *J. Atmos. Ocean. Technol.* 30, 2647–2661. doi: 10.1175/jtech-d-12-00241.1
- Fu, K.-H., Wang, Y.-H., St. Laurent, L., Simmons, H., and Wang, D.-P. (2012). Shoaling of large-amplitude nonlinear internal waves at Dongsha Atoll in the northern South China Sea. *Cont. Shelf Res.* 37, 1–7. doi: 10.1016/j.csr.2012.01.010
- Gong, G.-C., Lee Chen, Y.-L., and Liu, K.-K. (1996). Chemical hydrography and chlorophyll a distribution in the East China Sea in summer: implications in nutrient dynamics. *Cont. Shelf Res.* 16, 1561–1590. doi: 10.1016/0278-4343(96)00005-2
- Jan, S., and Chen, C. T. A. (2009). Potential biogeochemical effects from vigorous internal tides generated in Luzon Strait: a case study at the southernmost coast of Taiwan. *J. Geophys. Res. Oceans* 114:C04021.
- Li, D., Chou, W.-C., Shih, Y.-Y., Chen, G.-Y., Chang, Y., Chow, C.-H., et al. (2018). Elevated particulate organic carbon export flux induced by internal waves in the oligotrophic northern South China Sea. *Sci. Rep.* 8:2042.

DATA AVAILABILITY STATEMENT

The datasets generated for this study are available on request to the corresponding author.

AUTHOR CONTRIBUTIONS

W-CC, C-CH, and J-HT designed the experiments. W-CC and J-HT wrote the manuscript. K-CW and Y-HC performed the experiments and participated in discussions about the manuscript. T-YC, G-CG, F-KS, and CC participated in discussions and revised the manuscript. All of the authors reviewed the manuscript.

FUNDING

Funding was provided by the Ministry of Science and Technology of Taiwan grants #105-2119-M-019-004-, #106-2611-M-019-019-, and #107-2611-M-019-001-MY3 awarded to W-CC.

ACKNOWLEDGMENTS

We thank the crew of the R/V Ocean Researcher III for shipboard operations and water sampling and Rong-Wei Syu and Chin-Yo Yang for laboratory assistance.

SUPPLEMENTARY MATERIAL

The Supplementary Material for this article can be found online at: <https://www.frontiersin.org/articles/10.3389/fmars.2020.00511/full#supplementary-material>

- Liu, A.-K., Chang, Y.-S., Hsu, M.-K., and Liang, N.-K. (1998). Evolution of nonlinear internal waves in the East and South China Seas. *J. Geophys. Res. Oceans*. 103, 7995–8008. doi: 10.1029/97jc01918
- Liu, K.-K., Kao, S.-J., Hu, H.-C., Chou, W.-C., Hung, G.-W., and Tseng, C.-M. (2007). Carbon isotopic composition of suspended and sinking particulate organic matter in the northern South China Sea- from production to deposition. *Deep Sea Res. II* 54, 1504–1527. doi: 10.1016/j.dsr2.2007.05.010
- Pan, X.-J., Wong, G. T.-F., Shiah, F.-K., and Ho, T.-Y. (2012). Enhancement of biological productivity in the life phases of internal waves: observations in the northern South China Sea. *J. Oceanogr.* 68, 427–437. doi: 10.1007/s10872-012-0107-y
- Read, J., and Pollard, R. (2017). An introduction to the physical oceanography of six seamounts in the southwest Indian Ocean. *Deep Sea Res. II* 136, 44–58. doi: 10.1016/j.dsr2.2015.06.022
- Rogers, A. D. (1994). The biology of seamounts. *Adv. Mar. Biol.* 30, 305–350. doi: 10.1016/S0065-2881(08)60065-6
- Rowden, A. A., Dower, J. F., Schlacher, T. A., Consalvey, M., and Clark, M. R. (2010). Paradigms in seamount ecology: fact, fiction and future. *Mar. Ecol.* 31, 226–241. doi: 10.1111/j.1439-0485.2010.00400.x
- Sandstrom, H., and Elliott, J. (1984). Internal tide and solitons on the Scotian Shelf: A nutrient pump at work. *J. Geophys. Res. Oceans* 89, 6415–6426.
- Sharples, J., Moore, C. M., Hickman, A. E., Holligan, P. M., and Tweddle, J. F. (2009). Internal tidal mixing as a control on continental margin ecosystems. *Geophys. Res. Lett.* 36:L23603. doi: 10.1029/2009GL040683
- Takahashi, T., Olafsson, J., Goddard, J. G., Chipman, D. W., and Sutherland, S. C. (1993). Seasonal variation of CO₂ and nutrients in the high-latitude surface oceans: a comparative study. *Glob. Biogeochem. Cycles* 7, 843–878. doi: 10.1029/93gb02263
- Takahashi, T., Sutherland, S. C., Sweeney, C., Poisson, A., Metzl, N., and Tillbrook, B. (2002). Global sea-air CO₂ flux based on climatological surface ocean pCO₂, and seasonal biological and temperature effects. *Deep Sea Res. II* 49, 1601–1622. doi: 10.1016/S0967-0645(02)00003-6
- Villamaña, M., Mouriño-Carballido, B., Marañón, E., Cermeño, P., and Chouciño, P. (2017). Role of internal waves on mixing, nutrient supply and phytoplankton community structure during spring and neap tides in the upwelling ecosystem of Ría de Vigo (NW Iberian Peninsula). *Limnol. Oceanogr.* 62, 1014–1030. doi: 10.1002/lno.10482
- Wang, Y.-H., Dai, C.-F., and Chen, Y.-Y. (2007). Physical and ecological processes of internal waves on an isolated reef ecosystem in the South China Sea. *Geophys. Res. Lett.* 34, 1–5.
- Winn, C. D., Li, Y. H., Mackenzie, F. T., and Karl, D. M. (1998). Rising surface ocean dissolved inorganic carbon at the Hawaii Ocean Time-series site. *Mar. Chem.* 60, 33–47. doi: 10.1016/S0304-4203(97)00085-6
- Zhao, Z., Klemas, V., Zheng, Q., and Yan, X. H. (2004). Remote sensing evidence for baroclinic tide origin of internal solitary waves in the northeastern South China Sea. *Geophys. Res. Lett.* 31:L06302.

Conflict of Interest: The authors declare that the research was conducted in the absence of any commercial or financial relationships that could be construed as a potential conflict of interest.

Copyright © 2020 Tai, Chou, Hung, Wu, Chen, Chen, Gong, Shiah and Chow. This is an open-access article distributed under the terms of the Creative Commons Attribution License (CC BY). The use, distribution or reproduction in other forums is permitted, provided the original author(s) and the copyright owner(s) are credited and that the original publication in this journal is cited, in accordance with accepted academic practice. No use, distribution or reproduction is permitted which does not comply with these terms.